Magneto-optical properties of gallium-substituted yttrium iron garnets

P. Hansen and K. Witter
Philips GmbH Forschungslaboratorium Hamburg, D-2000 Hamburg 54, Federal Republic of Germany
(Received 5 May 1982)

The optical absorption α, the Faraday rotation θ_F, and the Faraday ellipticity ψ_F of epitaxial and flux-grown garnets of composition $\{Y_3\}[Fe_{2-x}Ga_x](Fe_{3-y}Ga_y)O_{12}$ with $0 \leq x+y \leq 2.95$ have been investigated. The wavelength dependence of α and θ_F was studied in the range $500 < \lambda < 1100$ nm at $T = 295$ K, revealing a strong reduction with increasing gallium content except for wavelengths between 600 and 700 nm. In this range the variation on $x+y$ for both θ_F and $|\psi_F|$ exhibits a maximum depending on temperature. Both quantities approximately approach zero at $x+y \approx 3$. The temperature dependence of θ_F and ψ_F was measured in the range $4.2\ \text{K} \leq T \leq T_C$ at $\lambda = 633$ nm. It can be described in terms of the sublattice magnetizations which were inferred from the fit of the molecular field theory to the measured saturation magnetization. The magneto-optical coefficients have been determined as a function of the gallium content.

I. INTRODUCTION

The magnetic properties such as the magnetization, the anisotropy, or the magnetostriction of gallium-substituted yttrium iron garnets have been studied extensively with respect to the concentration and temperature dependence and the effects arising from the distribution of the gallium ions on tetrahedral and octahedral sites.[1–5] The magneto-optical behavior of these materials, however, has not yet been investigated in detail except for some investigations concerning the Faraday rotation of special compositions[6–10] or for corresponding diamagnetic substitutions such as aluminum.[11]

The influence of diamagnetic dilutions on the Faraday rotation θ_F and the Faraday ellipticity ψ_F is of basic importance for the understanding of the iron transitions involved at different sublattices. This applies to the wavelength and the temperature dependence of these quantities being governed by the magneto-optical coefficients and the sublattice magnetizations. Further, those garnets with a high magneto-optical figure of merit θ_F/α which are attractive for device applications[12–14] contain an appreciable amount of gallium and thus their tailoring requires detailed information about the influence of this ion on θ_F and ψ_F.

Therefore, this paper is concerned with the behavior of θ_F and ψ_F for garnets of composition $\{Y_3\}[Fe_{2-x}Ga_x](Fe_{3-y}Ga_y)O_{12}$. The material parameters and the measured data are presented in Sec. II. In Sec. III the experimental data are compared with the theory yielding information about the concentration dependence of the magneto-optical constants.

II. EXPERIMENTAL RESULTS

A. Garnet material characterization

Epitaxial films and flux-grown crystals of composition

$$\{Y_{3-u}Pb_u\}[Fe_{2-x-v}Ga_xPt_v](Fe_{3-y}Ga_y)O_{12}$$

have been grown from $PbO\text{-}B_2O_3$—and $PbO\text{-}PbF_2\text{-}B_2O_3$—based fluxes, respectively. The epitaxial films were grown onto (111)-oriented ytterbium-substituted gadolinium gallium garnet substrates. The lead and platinum enter the lattice as impurities and are assumed to occupy dodecahedral and octahedral sites, respectively. The analysis data are compiled in Table I. The thickness of the films ranged between 2 and 46 μm. From the flux-grown crystals 100-μm-thick platelets were prepared.

The growth temperatures of the films ranged between 1000 and 1270 K which approximately correspond to the equilibrium temperatures T_e for the distribution of the gallium ions on the octahedral and tetrahedral sites.[3] For the flux-grown crystals in the as-grown state T_e can be assumed to be between 950 and 1050 K. The gallium distribution for different T_e values is presented in Fig. 1. The x,y data given in Table I are extracted from these dependences which were obtained from the fit of

TABLE I. Chemical analysis data of the investigated epitaxial garnet films (samples 1—9) and 100-μm-thick platelets cut from flux-grown crystals (samples 10—13) of composition $\{Y_{3-u}Pb_u\}[Fe_{2-x-v}Ga_xPt_v]$ $(Fe_{3-y}Ga_y)O_{12}$. Lead and platinum enter the lattice as impurities on dodecahredal and octahedral sites, respectively.

Sample no.	$x+y$	Impurities (Pb^{2+}, Pt^{4+}) u	v	Accuracy	Distribution[a] x	y
1	0	0.013	0.011		0	0
2	0.21	0.016	0.005		0.011	0.199
3	0.31	0.007	0.004	Ga^{3+}: ±0.01	0.017	0.293
4	0.47	0.010	0.005	Pt^{4+}: ±0.003	0.029	0.441
5	0.50	0.007	0.002	Pb^{2+}: ±0.003	0.034	0.466
6	0.89	0.008	0.004		0.074	0.816
7	0.93	0.006	0.002		0.079	0.951
8	1.15	0.007	0.001		0.114	1.036
9[b]	1.26	0.005	0.003		0.132	1.128
10	1.46				0.121	0.339
11	1.93	$\lesssim$0.01	<0.001		0.212	1.718
12	2.45				0.500	1.950
13	2.95					

[a]Distribution of gallium ions on octahedral and tetrahedral sites is inferred from the fit of the molecular-field theory to the measured saturation magnetization (Refs. 2 and 3).
[b]This sample contains 0.15 lanthanum per formula unit.

the molecular-field theory to the measured saturation magnetization for equilibrated samples.[3] The magnetization data for $T=4.2$ and 295 K are summarized in Table II. The calculation of the temperature dependence of M_s and the respective sublattice magnetizations is based on the results of Ref. 3 and the analysis data given in Table I.

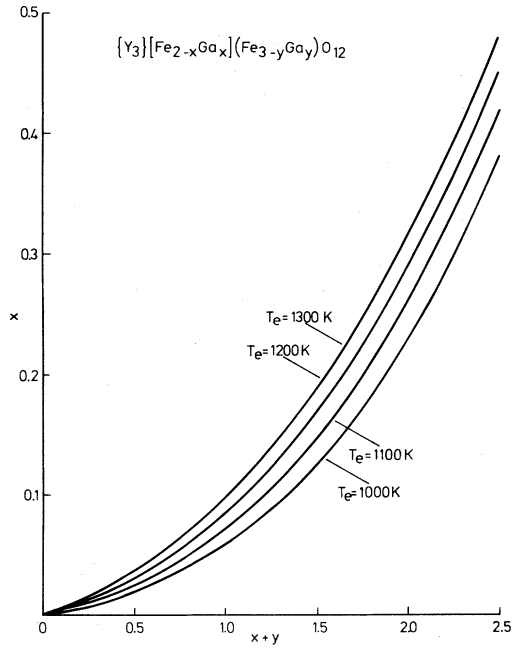

FIG. 1. Fraction of octahedral gallium ions vs total gallium content for different equilibrium temperatures according to Ref. 3.

B. Optical absorption

The optical absorption α was measured in a "Cary 17" spectrophotometer up to an optical density of 3. The measured values were corrected for the reflection losses employing the refractive index data for gallium-substituted garnets given in Ref. 15. The wavelength dependence of α at $T=295$ K is displayed in Fig. 2(a). The transitions have been assigned according to previous investigations.[16—19] The magnitude of α and the typical features of the spectra agree with literature data.[20—22] With increasing gallium content the spectrum is shifted towards longer wavelengths. In particular the shift of the octahedral transition ${}^6A_{1g}({}^6S)\rightarrow {}^4T_{1g}({}^4G)$ is about 40 nm. The absorption is reduced approximately by the wavelength-independent factor $(1-x/2)(1-y/3)$. The dependence of α on $x+y$ at selected wavelengths is shown in Fig. 2(b). Except for $\lambda=560$ nm a linear reduction of α with increasing $x+y$ is observed. At $y\approx 3$ $(x+y\approx 3.7)$ α approaches zero. For this case only the octahedral sublattice contributes to the absorption which for "one-sublattice" iron garnets is about 2 orders of magnitude lower than for "two-sublattice" iron garnets.[23,24]

TABLE II. Measured magnetic and magneto-optic (at $\lambda=633$ nm) data of the investigated garnets.

	$\mu_0 M_s$ (mT)		θ_F (deg cm^{-1})		$-\psi_F$ (deg cm^{-1})	
$x+y$	$T=4.2$ K	$T=295$ K	$T=4.2$ K	$T=295$ K	$T=4.2$ K	$T=295$ K
0	247	180	335	835	430	520
0.21	202	149	540	895	600	570
0.31	180	130	565	875	a	a
0.47	146	102	690	935	580	500
0.50	140	98	765	950	a	a
0.89	65	46	925	885	a	a
0.93	56	40	940	855	460	340
1.15	20	18	1025	765	425	260
1.26	3.3	1.2	1100	720	a	a
1.46	47	12	1105	645	400	210
1.93	93		970		215	
2.45	48		605		124	
2.95	7[b]		75[b]		15[b]	

[a]Measured data were omitted owing to the low accuracy caused by the small film thickness.
[b]Not saturated.

C. Faraday rotation

The temperature dependence of the Faraday rotation θ_F was measured with an optical hysteresigraph in fields up to 1.6×10^6 A/m.[25] The data were obtained from the hysteresis loops by extrapolation to zero field. For $x+y>1$ a compensation temperature of the saturation magnetization occurs[1,2] causing a sign change of θ_F. In the following figures this sign change has been omitted and the presented θ_F values correspond to a fixed direction of the sublattice magnetizations. The θ_F values for $T=4.2$ and 295 K are compiled in Table II.

The comparison of θ_F of different yttrium iron garnet samples[10,25] reveal a surprisingly high scatter yielding, at $T=4.2$ K, $\theta_F=280\pm50$ deg cm^{-1}, and at $T=295$ K, $\theta_F=790\pm30$ deg cm^{-1}. This may originate from different sources: (i) the error induced by that of the sample thickness ($\lesssim5\%$), (ii) the increased error of the θ_F measurements caused by internal reflections for very thin films ($<5\%$), and (iii) the strong effect of the varying lead content on the rotation[10,25,26] causing a change of θ_F by ∓80 deg cm^{-1} for $\Delta u=\pm0.01$ in the $Gd_3Fe_5O_{12}$ system.[10] These influences can explain the differences occurring at $T=295$ K, however, the scatter of the data at low temperatures indicate that a further contribution probably depending on the growth conditions affects the rotation as it is observed for distorted yttrium iron garnets.[27]

Further, it should be pointed out that the lead-free garnets exhibit a higher rotation which can be estimated from the Pb contribution $\Delta\theta_F(\mathrm{Pb})/u=-7700$ deg cm^{-1} at $\lambda=633$ nm and $T=295$ K,[10,25,26] and the analysis data, provided the influence of the lead ions on the magneto-optic properties is not much different in these garnets as compared to the $Gd_3Fe_5O_{12}$ garnets.

The dependence of θ_F on the gallium content at $\lambda=633$ nm is shown in Fig. 3 for three temperatures. The concentrations where $\theta_F=0$ are inferred from the concentration dependence of the Curie temperature.[3] For temperatures $T\lesssim400$ K a maximum of θ_F is observed owing to the reduction of the tetrahedral contribution and the superexchange interaction causing a decrease of T_C. Thus, for tetrahedral substitutions up to $x+y\approx1.1$ the rotation at $T=295$ K is higher than that of yttrium iron garnet whereas the corresponding absorption is lower. At $x+y\approx3$ the rotation at $T=4.2$ K approaches zero in agreement with the magnetization.[1]

The variation of θ_F with temperature at $\lambda=633$ nm is presented in Figs. 4(a) and 4(b). For samples 3 and 6 the curves overlap with others in a wide range and therefore have been omitted. For $x+y\lesssim0.95$ a maximum of θ_F occurs which is shifted towards lower temperatures with increasing gallium content. At high $x+y$ the octahedral sublattice predominates resulting in a rotation decreasing monotonically with T. The theoretical curves are discussed in Sec. III.

The wavelength dependence of θ_F was measured with an optical hysteresigraph operating only at $T=295$ K. θ_F vs λ is displayed in Fig. 5 for some films of suitable thickness. The dotted line is taken

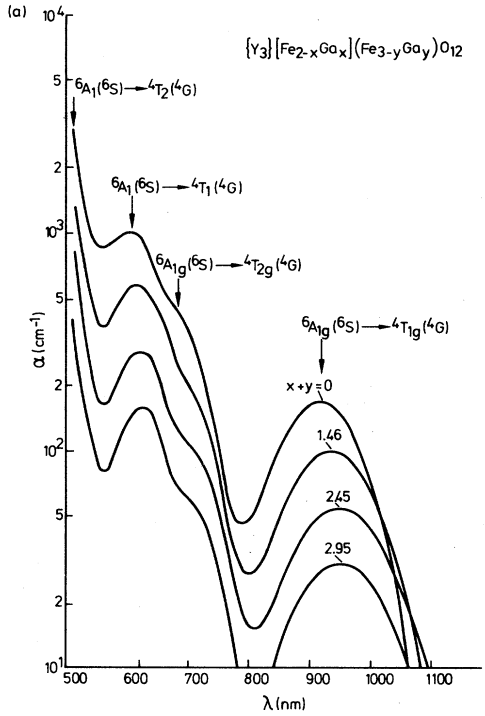

FIG. 2. Optical absorption vs (a) wavelength in the range of crystal-field transitions for different gallium contents, and (b) gallium content at different wavelengths.

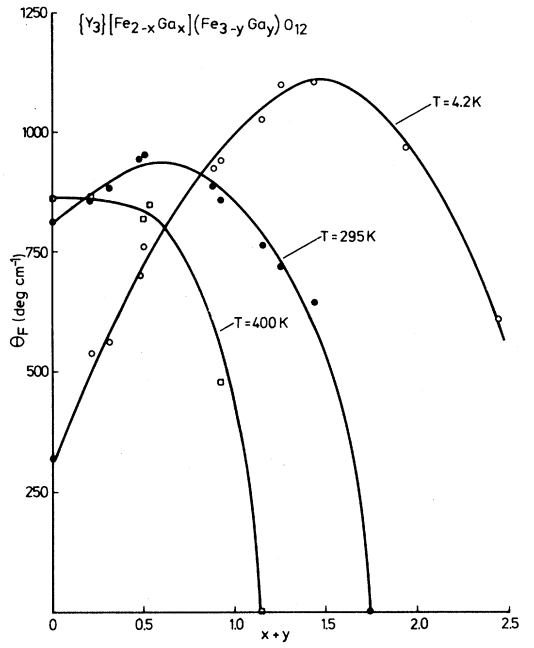

FIG. 3. Faraday rotation at $\lambda = 633$ nm vs gallium content for different temperatures.

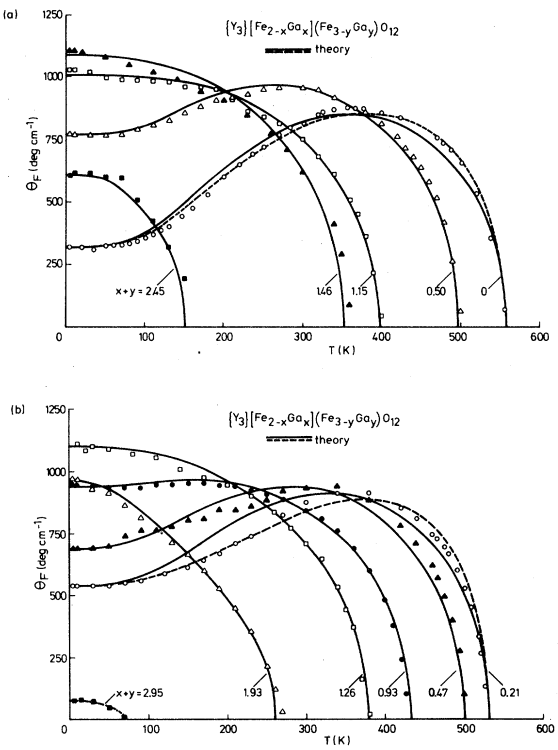

FIG. 4. (a) and (b): Faraday rotation at $\lambda = 633$ nm vs temperature for different gallium contents. Solid lines represent the calculated dependence according to Eq. (3a). Dashed lines were calculated from Eq. (2a).

from Ref. 21. Around the maximum at $\lambda = 530$ nm and for longer wavelengths ($\lambda \gtrsim 700$ nm) the gallium substitution reduces the rotation approximately by the same factor. In the range $600 \lesssim \lambda \lesssim 700$ nm

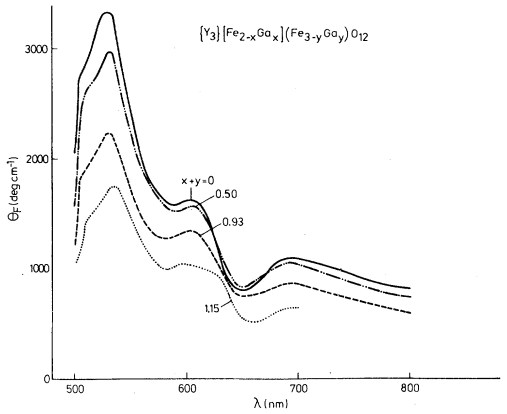

FIG. 5. Faraday rotation vs wavelength in the range of crystal-field transitions for different gallium contents at $T=295$ K. Dotted line is taken from Ref. 21.

the behavior of θ_F is more complex yielding a concentration dependence as shown in Fig. 3.

D. Faraday ellipticity

The Faraday ellipticity was measured with the same equipment used for the θ_F measurements except that a quarter-wave plate was added behind the sample and roughly adjusted with its birefringent axis parallel to the incident polarization. This plate transforms the Faraday ellipticity ϵ_F directly into a rotation $\psi_F L = \text{arctanh}\epsilon_F$ of the azimuth detectable by the corresponding rotation of the analyzer until minimum transmitted intensity is reached. L denotes the thickness of the films. The accuracy of the measurements is affected by the birefringence of the windows of the optical cryostat and the oven[25] and that of the substrates. The given ψ_F data were derived from the measured hysteresis loops by extrapolation to zero field. For $T=4.2$ and 295 K the

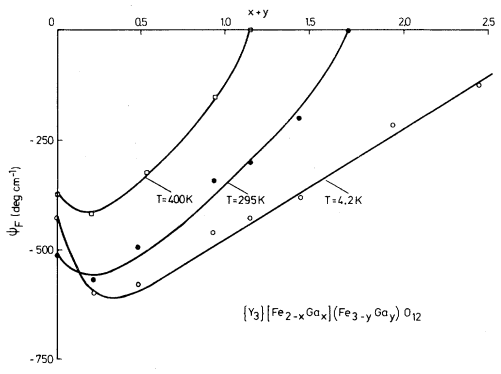

FIG. 6. Faraday ellipticity at $\lambda=633$ nm vs gallium content for different temperatures.

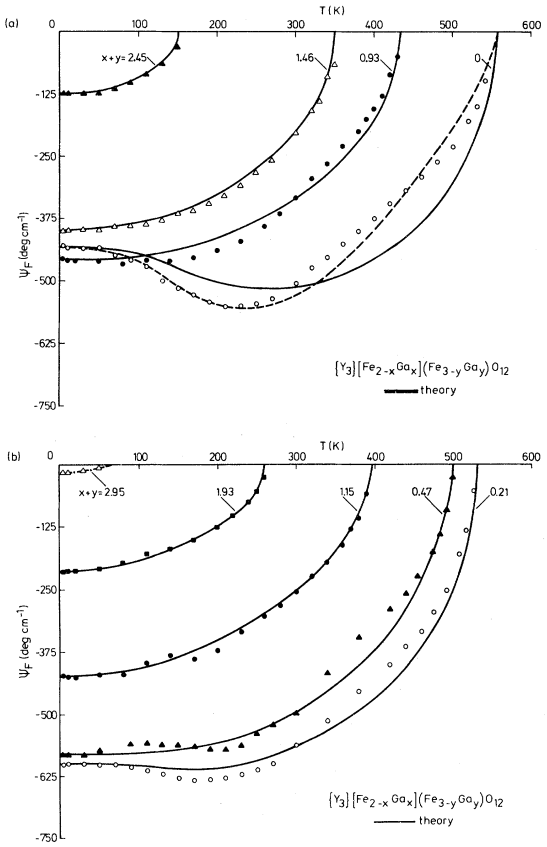

FIG. 7. (a) and (b): Faraday ellipticity at $\lambda=633$ nm vs temperature for different gallium contents. Solid lines represent the calculated dependence according to Eq. (3b). Dashed line in (a) was calculated from Eq. (2b).

data are summarized in Table II. For the thin films the measured data are not very accurate and therefore have been omitted in Table II.

As in the case of the rotation the lead impurities cause a significant influence on the ψ_F values. In lead-substituted $Gd_3Fe_5O_{12}$ garnets[25] the lead contribution amounts to $\Delta\psi_F(\text{Pb})/u \approx -6000$ deg cm^{-1} at $\lambda=633$ nm and $T=295$ K corresponding to ∓ 60 deg cm^{-1} for lead variations of $\Delta u = \pm 0.01$. A comparable effect of the lead is expected for the investigated gallium-substituted iron garnets. In particular, the ψ_F values for yttrium iron garnet given in Table II differ slightly from those reported in Ref. 25 which has to be attributed to the difference in the Pb-impurity content.

The concentration dependence of ψ_F at $\lambda=633$ nm is displayed in Fig. 6 for three temperatures. ψ_F shows a minimum at much lower gallium substitutions as compared to the position where θ_F reaches the maximum value. For $x+y\approx 3$ the el-

lipticity at $T=4.2$ K almost disappears in accordance with θ_F and M_s. The variation of ψ_F with temperature at $\lambda=633$ nm is shown in Figs. 7(a) and 7(b). A minimum is observed in the low-temperature range for low Ga content. For high Ga content a one-sublattice behavior appears similar to the θ_F case.

III. DISCUSSION

A. Theory

The magneto-optical effects originate from the magnetic and electric dipole transitions. Both can be expressed in terms of the sublattice magnetizations.[25,28–30] Since the rotation and the ellipticity are odd functions with respect to a sign change of the magnetization

$$\theta_F(\vec{\mathrm{M}})=-\theta_F(-\vec{\mathrm{M}}) , \quad \psi_F(\vec{\mathrm{M}})=-\psi_F(-\vec{\mathrm{M}}) , \tag{1}$$

an expansion in powers of the sublattice magnetizations yields

$$\theta_F=\theta_F^0[1+pM_a(T)M_d(T)+\cdots] , \tag{2a}$$

$$\psi_F=\psi_F^0[1+qM_a(T)M_d(T)+\cdots] , \tag{2b}$$

where $M_a(T)$ and $M_d(T)$ are the octahedral and tetrahedral sublattice magnetizations, respectively. θ_F^0 and ψ_F^0 represent the linear terms in $M_a(T)$ and $M_d(T)$,

$$\theta_F^0=AM_a(T)+DM_d(T) , \tag{3a}$$

$$\psi_F^0=aM_a(T)+dM_d(T) , \tag{3b}$$

which are frequently used to describe the temperature dependence of the rotation and the ellipticity. A,a and D,d are the magneto-optical coefficients depending on frequency. These coefficients are composed of an electric and a magnetic dipole transition coefficient as, e.g.,

$$A=-A_e-A_m , \quad D=D_e+D_m , \tag{4}$$

where $A_m=D_m=9.57$ deg cm$^{-1}\mu_B^{-1}$ at $\lambda=633$ nm, provided the sublattice magnetizations are expressed in Bohr magnetons per two formula units.[10] p and q are the corresponding constants of the third-order magnetization terms. The magneto-optical coefficients can be extracted from the fit of these equations to the experimental data.

B. Faraday rotation

In the measured wavelength range θ_F is governed by both the tetrahedral and octahedral crystal-field transitions.[16–19] The almost wavelength-independent reduction of the absorption [Fig. 2(a)] by Ga dilutions suggests that pairs of tetrahedral and octahedral Fe^{3+} ions are involved.[19] The theory predicts a variation of θ_F with respect to composition and temperature according to Eqs. (2) or (3). Diamagnetic dilutions thus affect θ_F through both the magneto-optical coefficients and the sublattice magnetizations. In particular, for $Y_3Fe_5O_{12}$ at $\lambda=633$ nm, the octahedral and tetrahedral contributions are large and of comparable magnitude as shown in Table III and, thus, a gallium substitution leads to an increase of θ_F (Fig. 3) owing to the reduction of the tetrahedral contribution via that of M_d. For higher substitutional levels the reduction of the exchange interaction causes a decrease of θ_F approaching zero if the Fe^{3+} ions of the tetrahedral sublattice have been completely replaced by Ga^{3+} ions. At longer wavelengths there is no maximum observed in the concentration dependence of θ_F in agreement with results reported for aluminium-substituted garnets at $\lambda=1.15$ μm.[11] This can be explained by the reduction of the significantly larger octahedral coefficient at these wavelengths which compensates the reduction of the tetrahedral contribution.

The temperature dependence of θ_F calculated from Eq. (3a) with temperature-independent

TABLE III. Sublattice contributions of the magnetic and electric dipole transitions to the Faraday rotation at $\lambda=633$ nm for yttrium iron garnet. Magneto-optical coefficients are related to the rotation according to Eqs. (3) and (4) where the sublattices are expressed in Bohr magnetons per two formula units.

T (K)	A_eM_a (deg cm^{-1})	A_mM_a (deg cm^{-1})	D_eM_d (deg cm^{-1})	D_mM_d (deg cm^{-1})	θ_F (deg cm^{-1})
4.2	−9878	191	−9640	288	335
295	−8840	171	−8076	242	835
400	−7396	143	−6597	197	853

magneto-optical coefficients is shown in Figs. 4(a) and 4(b). The sublattice magnetizations were inferred from Ref. 3. Except for samples 2 and 4 a good agreement between the experimental and theoretical variation is achieved. For yttrium iron garnet minor deviations occur which have been attributed to a temperature dependence of the magneto-optical coefficients.[31] However, if a higher-order term is taken into account according to Eq. (2a) this discrepancy can be removed, too. This is demonstrated by the dashed line in Figs. 4(a) and 4(b). The magnitudes of A and D are significantly affected by the introduction of a third-order term which contributes about 15% to the rotation. For higher gallium contents this term becomes less important except for the range around the compositional compensation point.

The magneto-optical coefficients were deduced by adjusting Eq. (3a) to the experimental data at two temperatures T_1 and T_2 leading to the equation

$$A=\frac{\theta_F(T_1)M_d(T_2)-\theta_F(T_2)M_d(T_1)}{M_a(T_1)M_d(T_2)-M_a(T_2)M_d(T_1)}\,, \qquad (5)$$

and a corresponding one for D. With increasing gallium content the denominator passes through zero owing to the compositional compensation point of this system. The induced singularity of A and D is shown in Fig. 8. The symbols marked with a cross were calculated from θ_F values taken from Figs. 3 and 4 (solid lines). Physically this singularity appears to be meaningless suggesting that the linear relationship of θ_F in terms of the sublattice magnetizations is not correct at least in the neighborhood of the compensation point. The same difficulty arises for the anisotropy and magnetostriction constants.[5] This problem has not yet been solved. The inclusion of further terms, e.g., third-order terms, generates the difficulty that the accuracy of the experimental data must be extremely high to extract fairly reliable values for the corresponding constants.

C. Faraday ellipticity

The influence of the gallium substitution on the Faraday ellipticity is similar to that on the rotation. The concentration dependence of ψ_F at $\lambda=633$ nm exhibits a minimum (Fig. 6) and the temperature dependence changed with increasing gallium content from that of yttrium iron garnet with a minimum in the low-temperature range to a monotonically increasing dependence of ψ_F as it is expected for a ferromagnet with one dominating sub-

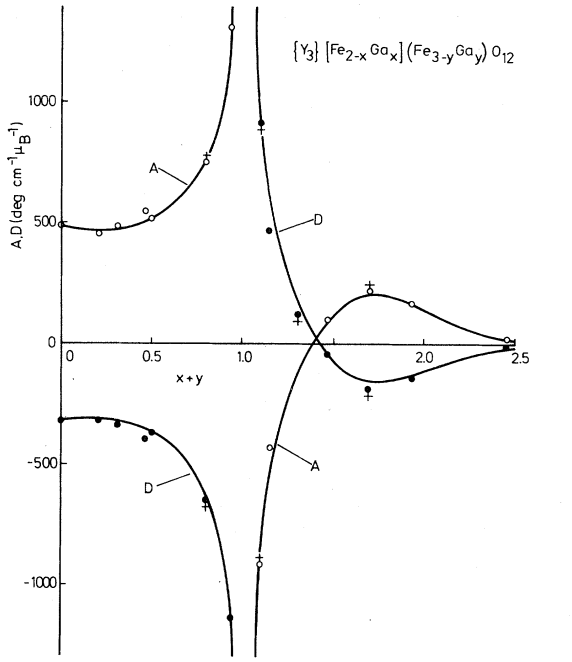

FIG. 8. Magneto-optical coefficients at $\lambda=633$ nm vs gallium content. Singularity is caused by the compositional compensation point of the magnetization. Symbols marked with a cross were calculated from θ_F data taken from Figs. 3 and 4 (solid lines).

lattice [Figs. 7(a) and 7(b)].

The comparison of the experimental data with the theoretical dependence is shown in Figs. 7(a) and 7(b). The solid lines were calculated from Eq. (3b) with temperature-independent coefficients and lead to a good fit for higher gallium contents. For small substitutional levels and in particular for yttrium iron garnet significant deviations between theory and experiment occur which can be reduced considerably if a third-order term in the sublattice magnetizations is taken into account using Eq. (2b). The result is shown by the dashed line in Fig. 7(a) representing a satisfactory fit of the experimental data. Similar to the case of the rotation this raises the question whether third-order terms or a temperature dependence of the linear coefficients have to be used to describe the experimental temperature variation.

The magneto-optical coefficients extracted from the fit of the measured temperature dependence of ψ_F are compiled for some samples in Table IV. The sign of the octahedral and tetrahedral coefficients are reversed as compared to that of A and D due to the negative sign of ψ_F. The accuracy of the coefficients is much less than indicated in Table IV; however, the given numbers offer the possibility for the recalculation or interpolation of the theoretical

TABLE IV. Magneto-optical coefficients of the Faraday ellipticity at $\lambda=633$ nm.

Sample no.	a (deg cm$^{-1}\mu_B^{-1}$)	d (deg cm$^{-1}\mu_B^{-1}$)
1	−130.9	72.5
2	−77.1	33.3
4	−53.3	18.7
7	53.3	−69.0
8	212.0	−243.6
10	7.3	−28.1
11	−22.5	12.3

curves. As a function of $x+y$ the coefficients pass through a singularity caused by the compensation point of M_s similar to the variation of A and D. The solution of this problem requires further investigations. A plot of a and d versus $x+y$ has not been given since much less data are available as compared to the θ_F case.

IV. CONCLUSIONS

The diamagnetic dilution of the tetrahedral sublattice of yttrium iron garnet by gallium substitution causes strong changes of the optical and magneto-optical properties. With increasing gallium content for the optical absorption an approximately wavelength-independent reduction is observed in the range $500 \lesssim \lambda \lesssim 1100$ nm. The Faraday rotation and ellipticity are also characterized by a reduction except for wavelengths between 600 and 700 nm where θ_F and $|\psi_F|$ increase passing through a maximum at moderate Ga contents. The temperature dependence at $\lambda=633$ nm can be described by temperature-independent magneto-optical coefficients for both θ_F and ψ_F. The temperature dependence of the sublattice magnetizations were inferred from the fit of the molecular-field theory to the measured saturation magnetization. Deviations between theory and experiment for low gallium contents can be removed by adding a third-order term in the sublattice magnetization to the theoretical expression. The presence of higher-order terms is also indicated by the concentration dependence of the optical absorption.

The extracted magneto-optical coefficients exhibit a singularity as a function of the gallium content owing to the compositional compensation point of the magnetization.

ACKNOWLEDGMENTS

The authors would like to thank I. Bartels and W. Tolksdorf for the growth and preparation of the investigated garnets, P. Willich for the chemical analysis, V. Doormann for measuring the Faraday spectra, and J. Schuldt and M. Rosenkranz for technical assistance. Helpful discussions with H. Heitmann and J.-P. Krumme are gratefully acknowledged.

[1]S. Geller, J. A. Cape, G. P. Espinosa, and D. H. Leslie, Phys. Rev. 148, 522 (1966).
[2]P. Hansen, P. Röschmann, and W. Tolksdorf, J. Appl. Phys. 45, 2728 (1974).
[3]P. Röschmann and P. Hansen, J. Appl. Phys. 52, 6257 (1981).
[4]P. Hansen, J. Appl. Phys. 45, 3638 (1974).
[5]P. Hansen, in *Physics of Magnetic Garnets*, edited by A. Paoletti (North-Holland, New York, 1978), p. 56.
[6]H. Matthews, S. Singh, and R. C. LeCraw, Appl. Phys. Lett. 7, 165 (1965).
[7]Berdennikova and R. V. Pisarev, Izv. Akad. Nauk. SSSR, Ser. Fiz. 38, 2419 (1974); [Bull. Acad. Sci. USSR, Phys. Ser. 38, 156 (1974)].
[8]Š. Višňovský, V. Prosser, M. Zvára, and P. Polívka, Phys. Status Solidi A 26, 513 (1974).
[9]P. Cœre, D. Challeton, J. Daval, J. P. Jadot, and J. C. Peuzin, Rev. Phys. Appl. 10, 379 (1975).
[10]P. Hansen, H. Heitmann, and K. Witter, Phys. Rev. B 23, 6085 (1981).
[11]H. LeGall, J. Ostorero, H. Makram, and J. M. Desvignes, IEEE Trans. Magn. 17, 3229 (1981).
[12]B. Hill and K.-P. Schmidt, Phil. J. Res. 33, 211 (1978).
[13]B. Hill and K.-P. Schmidt, SID J. 10, 80 (1979).
[14]J. J. Krebs, W. G. Maisch, G. A. Prinz, and D. W. Forester, IEEE Trans. Magn. 16, 1179 (1980).
[15]V. A. Odarich, V. A. Ruban, and P. F. Gul'schuk, Fiz. Tverd. Tela (Leningrad) 20, 3477 (1978) [Sov. Phys.—Solid State 20, 2010 (1978)].
[16]D. L. Wood and J. P. Remeika, J. Appl. Phys. 38, 1038 (1967).
[17]G. B. Scott, D. E. Lacklison, and J. L. Page, Phys. Rev. B 10, 971 (1974).
[18]S. H. Wemple, S. L. Blank, J. A. Seman, and W. A. Biolsi, Phys. Rev. B 9, 2134 (1974).
[19]G. B. Scott, in *Physics of Magnetic Garnets*, edited by A. Paoletti (North-Holland, New York, 1978), p. 445.
[20]A. V. Antonov and A. I. Belyaeva, Fiz. Tverd. Tela (Leningrad) 14, 1023 (1972) [Sov. Phys.—Solid State 14, 876 (1972)].
[21]D. E. Lacklison, G. B. Scott, H. I. Ralph, and J. L. Page, IEEE Trans. Magn. 9, 457 (1973).

[22]P. K. Larsen and J. M. Robertson, J. Appl. Phys. 45, 2867 (1974).
[23]G. S. Krinshik, V. D. Gorbunova, V. S. Gushchin, and B. V. Mill, Fiz. Tverd. Tela (Leningrad) 22, 264 (1980) [Sov. Phys.—Solid State 22, 156 (1980)].
[24]G. S. Krinshik, M. Kučera, V. D. Gorbunova, and V. S. Gushchin, Fiz. Tverd. Tela (Leningrad) 23, 405 (1981) [Sov. Phys.—Solid State 23, 229 (1981)].
[25]P. Hansen, M. Rosenkranz, and K. Witter, Phys. Rev. B 25, 4396 (1982).
[26]P. Hansen, W. Tolksdorf, and K. Witter, IEEE Trans. Magn. 17, 3211 (1981).
[27]H. Heitmann and P. Hansen, J. Appl. Phys. (in press).
[28]W. A. Crossley, R. W. Cooper, J. L. Page, and R. P. van Stapele, Phys. Rev. 181, 896 (1969).
[29]H. LeGall, J. Phys. (Paris) Colloq. 1, Suppl. 32, 590 (1971).
[30]W. Wettling, Appl. Phys. 6, 367 (1975).
[31]G. Abulafya and H. LeGall, Solid State Commun. 11, 629 (1972).